# THE EFFECT OF EQUILIBRIUM FLOW ON THE STABILITY OF TEARING MODES IN THE REVERSED-FIELD PINCH

**R. GATTO, P. W. TERRY, C. C. HEGNA**

DEPARTMENT OF PHYSICS

UNIVERSITY OF WISCONSIN-MADISON

MADISON, WI 53706 USA

Poster 2D09 of the International Sherwood Fusion Theory Meeting,

April 2-4 2001, Santa Fe, NM, USA

# OUTLINE

## (I) MOTIVATIONS AND GOAL

- Shear flow in high-confinement discharges
  - Tokamak
  - Reversed-field pinch
- Goal: $\triangle'$ calculation with shear flow localized away from rational surface

## (II) STABILITY OF TEARING MODES

- Ideal Kink Equation
- Stability parameter $\triangle'$

## (III) STABILITY WITH FLOW

- Potential energy
- Stabilization conditions

## (IV) NUMERICAL RESULTS

## (V) CONCLUSIONS AND FUTURE WORK

# PART I

## MOTIVATIONS AND GOAL

### Shear flow in high-confinement discharges

- $E \times B$ shear flow seems to be a universal feature of improved confinement regimes in magnetically confined plasmas
- Tokamak

  ∘ Fluctuations are predominantly electrostatic and of short wavelength

  ∘ Shear flow suppresses turbulence and reduces transport *[H. Biglari, P. H. Diamond and P. W. Terry, Phys. Fluids, 3, 1, (1990)]*
- Reversed-field pinch

  ∘ Fluctuations are predominantly magnetic and global

  ∘ The spontaneous enhanced confinement regime observed in the Madison Symmetric Torus (MST) is characterized by a self-induced $E_r$ which creates a region of strong shear flow ($V_z = E_r B_z / B_0^2$) near the edge of the plasma *[Chapman, et al., Phys. Plasmas 5, p.1848, (1998)]*

∘ *Both local electrostatic and global magnetic fluctuations are reduced*

# Goal

- Perform $\triangle'$ calculations with a region of shear flow localized away from the rational surface ⇒ *study the effect of a localized region of shear flow on the stability of tearing modes in the reversed-field pinch*

- Main conclusion: A region of shear flow localized at the edge of the reversed-field pinch plasma further *destabilizes* core $m = 1$ global tearing modes.

# PART I

# STABILITY OF TEARING MODES

## Ideal Kink Equation

- Incompressible ideal MHD system

$$\rho = \text{const.} \,, \qquad \boldsymbol{\nabla} \cdot \mathbf{V} = 0 \,, \qquad \boldsymbol{\nabla} \cdot \mathbf{B} = 0 \,,$$

$$\rho \left[ \frac{\partial \mathbf{V}}{\partial t} + (\mathbf{V} \cdot \boldsymbol{\nabla})\, \mathbf{V} \right] + \boldsymbol{\nabla} p - \mathbf{J} \times \mathbf{B} = 0 \,, \qquad \mathbf{E} = -\mathbf{V} \times \mathbf{B} \,,$$

$$\mu_0 \mathbf{J} = \boldsymbol{\nabla} \times \mathbf{B} \,, \qquad \frac{\partial \mathbf{B}}{\partial t} = -\boldsymbol{\nabla} \times \mathbf{E} \,.$$

- In cylindrical geometry, and assuming

$$\mathbf{B}(r,\theta,t) = \overbrace{\left[ B_\theta(r) \hat{\boldsymbol{\theta}} + B_z(r) \hat{\mathbf{z}} \right]}^{\text{equilibrium}} + \overbrace{\tilde{\mathbf{B}}(r) \exp[i(m\theta + kz + \omega t)]}^{\text{perturbation}}$$

$$\mathbf{V}(r,\theta,t) = \left[ V_\theta(r) \hat{\boldsymbol{\theta}} + V_z(r) \hat{\mathbf{z}} \right] + \tilde{\mathbf{V}}(r) \exp[i(m\theta + kz + \omega t)] \,,$$

we obtain a second order o.d.e. for $\tilde{B}_r(r)$:

$$\frac{d^2 \tilde{B}_r(r)}{dr^2} + C(r;\omega)\, \frac{d\tilde{B}_r(r)}{dr} + D(r;\omega)\, \tilde{B}_r(r) = 0 \,.$$

- Defining:

$$V^2 = V_\theta^2 + V_z^2 \ , \qquad B^2 = B_\theta^2 + B_z^2 \ .$$

$$G = \mathbf{k}\cdot\mathbf{V} \ , \qquad F = \mathbf{k}\cdot\mathbf{B}$$

$$\Omega = \omega + G \ , \qquad \Sigma^2 = \mu_0\rho\Omega^2 - F^2 \ ,$$

$$M_{pq} = p\, m^2 + q\, k_z^2 r^2 \ , \qquad H = -\frac{r^3}{M_{11}}\frac{\Sigma^2}{F^2}$$

$$\mathcal{F} = -\frac{m}{r}B_\theta\left[\frac{M_{11}}{m^2}\frac{F^2}{\Sigma^2} + \frac{k_z^2 r^2}{m^2}\right] + k_z B_z \ ,$$

($p, q$ are positive integers), the coefficients read

$$C(r) = \frac{1}{H}\frac{dH}{dr} \qquad D(r) = g(r) - \frac{1}{HF}\frac{d}{dr}\left(H\frac{dF}{dr}\right) \ ,$$

where

$$\begin{aligned} g(r) &= -\frac{m^2-1}{r^2} \\ &- \frac{1}{F^2}\frac{k_z^2}{r}\left[\!\left[-\frac{F^2}{\Sigma^2}2\mu_0\frac{dp}{dr} + rF^2 + F\frac{2\left\{rk_zB_z - mB_\theta\left[2(-\mathcal{F}F/\Sigma^2)-1\right]\right\}}{M_{11}}\right]\!\right] \\ &+ \frac{F}{\Sigma^4}\frac{4\mu_0\rho k_z^2 V_\theta}{r^2}\left(V_\theta F - 2B_\theta\Omega\right) \\ &+ \frac{2\mu_0\rho}{r^3\Sigma^2}\left\{r^2\left[\frac{d\Omega}{dr}\left(\Omega - \frac{m}{r}V_\theta\right) + \frac{dV_\theta}{dr}\left(\frac{M_{11}}{r^2}V_\theta - \frac{m}{r}\Omega\right)\right] + mV_\theta\left(\Omega\frac{M_{13}}{M_{11}} - \frac{m}{r}V_\theta\right)\right\} \ . \end{aligned}$$

## Stability parameter

- The outer region equation is solved numerically in the $\omega = 0$ approximation to evaluate $\Delta'$ ($x \equiv r - r_s$):

$$\Delta' \equiv \frac{1}{\tilde{B}_r(0)} \left[ \left. \frac{d\tilde{B}_r}{dx} \right|_{x \to 0^+} - \left. \frac{d\tilde{B}_r}{dx} \right|_{x \to 0^-} \right] .$$

  - Procedure is conventional: matching of the numerical solution in the ideal outer region with the series solution near the rational surface.

# PART III

# STABILITY CONSIDERATION

## Potential energy

- New dependent variable

$$\psi = \frac{r(1-\Upsilon^2)^{1/2}}{M_{11}^{1/2}}\tilde{B}_r$$

where

$$\Upsilon^2 = \left(\frac{\mathbf{k}\cdot\mathbf{U}}{\mathbf{k}\cdot\mathbf{V}_A}\right)^2$$

is the ratio of kinetic to magnetic energy [$\mathbf{U} \equiv \mathbf{V}(r) - \mathbf{V}(r_s)$, where $r_s$ is the location of the rational surface, and $\mathbf{V}_A = \mathbf{B}/(\mu_0\rho)^{1/2}$]

- Ideal kink equation recast as $[K^2 = m^2/r^2 + k_z^2]$

$$\frac{1}{r}\frac{d}{dr}\left(r\frac{d\psi}{dr}\right) - U\ \psi = K^2\psi$$

- The "potential energy" $U$ is

$$\begin{aligned}
U(r) &= -\frac{1}{r^2} + \frac{1}{F}\left(\frac{M_{31}}{rM_{11}}\frac{dF}{dr} + \frac{d^2F}{dr^2}\right) + \frac{m^2(m^2 - 2k_z^2r^2)}{M_{11}^2r^2} \\
&+ \frac{k_z^2}{rF^2}\left\{2\mu_0\frac{(dp/dr)}{(1-\Upsilon^2)}\right. \\
&\left. +\frac{2F}{M_{11}}\left[rk_zB_z + mB_\theta\left(\frac{2k_zr}{m}\frac{k_zB_\theta - (m/r)B_z}{F(1-\Upsilon^2)} - \frac{2M_{11}B_\theta}{mrF(1-\Upsilon^2)^2} + 1\right)\right]\right\} \\
&- \frac{2\mu_0\rho k_z^2}{r^2F^2(1-\Upsilon^2)}\left[\frac{2V_\theta}{(1-\Upsilon^2)}\left(V_\theta - \frac{2\Omega B_\theta}{F}\right) - \frac{r}{2}\left(\frac{dV^2}{dr} + 4\frac{m}{M_{11}}V_\theta\Omega\right)\right] \\
&- \frac{1}{2(1-\Upsilon^2)}\left\{\frac{d^2\Upsilon^2}{dr^2} + \left[\frac{(d\Upsilon^2/dr)}{2(1-\Upsilon^2)} + \frac{M_{31}}{rM_{11}} + \frac{1}{F^2}\frac{dF^2}{dr}\right]\frac{d\Upsilon^2}{dr}\right\}.
\end{aligned}$$

# Stabilization conditions

- Multiplying by $\psi$, applying the operators $\lim_{\epsilon\to 0}\int_0^{r_s-\epsilon} dr$ and $\lim_{\epsilon\to 0}\int_{r_s+\epsilon}^{a} dr$ and adding the two resulting equations we obtain

$$r_s\,\Delta' = -\left\{\overline{\int}_0^a dr\; r\left[\left(\frac{d\psi/dr}{\psi_s}\right)^2 + K^2\;\left(\frac{\psi}{\psi_s}\right)^2\right]\right\}$$
$$-\overline{\int}_0^a dr\; r\;\overbrace{(U_0+U_1)}^{U}\left(\frac{\psi}{\psi_s}\right)^2$$

where $\psi_s = \psi(r_s)$ and

$$\overline{\int}_0^a dr \equiv \lim_{\epsilon\to 0}\left(\int_0^{r_s-\epsilon} dr + \int_{r_s+\epsilon}^{a} dr\right)\ ,$$

- $U_0$ is the flowless part of the potential

$$\begin{aligned} U_0 \;&=\; -\frac{1}{r^2} + \frac{1}{F}\left(\frac{M_{31}}{rM_{11}}\frac{dF}{dr} + \frac{d^2F}{dr^2}\right) + \frac{m^2(m^2-2k_z^2r^2)}{M_{11}^2r^2} \\ &+\; \frac{k_z^2}{rF^2}\left\{2\mu_0\frac{dp}{dr}\right. \\ &+\; \left.\frac{2F}{M_{11}}\left[rk_zB_z - mB_\theta\left(-\frac{2k_zr}{m}\frac{k_zB_\theta-(m/r)B_z}{F} + \frac{2M_{11}B_\theta}{mrF} - 1\right)\right]\right\} \end{aligned}$$

- $U_1 \equiv U - U_0$ is the remaining part of the potential due to the presence of a nonzero flow.

- $U_1$ can be conveniently divided into two contributions,

$$U_1(r) = U_{1,1} + U_{1,2} \ ,$$

where

$$U_{1,1} = -\left(\frac{1}{F}\frac{dF}{dr} + \frac{M_{31}}{2rM_{11}}\right)\frac{1}{(1-\Upsilon^2)}\frac{d\Upsilon^2}{dr} - \frac{1}{4(1-\Upsilon^2)^2}\left(\frac{d\Upsilon^2}{dr}\right)^2 - \frac{1}{2(1-\Upsilon^2)}\frac{d^2\Upsilon^2}{dr^2} \ ,$$

$$U_{1,2} = \frac{2k_z^2}{rF^2}\left\{\left[\mu_0\frac{dp}{dr} + \frac{2rk_zB_\theta(k_zB_\theta - (m/r)B_z)}{M_{11}} - \frac{2B_\theta^2}{r}\frac{(2-\Upsilon^2)}{(1-\Upsilon^2)}\right]\Upsilon^2 - \left[\frac{2V_\theta}{r(1-\Upsilon^2)}\left(V_\theta - \frac{2\Omega B_\theta}{F}\right) - \frac{1}{2}\left(\frac{dV^2}{dr} + 4\frac{m}{M_{11}}V_\theta\Omega\right)\right]\mu_0\rho\right\}\frac{1}{(1-\Upsilon^2)} \ .$$

- The flow contribution to $\triangle'$ is

$$\mathcal{I} \equiv \int_0^a dr\ r\ \left(\frac{\psi}{\psi_s}\right)^2 U_1$$

◦ Global condition: *the flow is stabilizing/ destabilizing if* $\mathcal{I}$ *is greater/less than 0*

◦ Local condition: *the flow is locally stabilizing/destabilizing if* $U_1$ *is positive/negative*

- Comment: $\mathcal{I}$ depends on $U_1$ *and* the weighting function $r(\psi/\psi_s)^2$, thus a knowledge of the eigenfunction $\tilde{B}_r$ is needed in order to calculate $\mathcal{I}$. However, since the weighting function is *positive definite*, consideration of the "potential energy" $U_1$ alone (which depends only on equilibrium profiles) can give trend information on the influence of the flow on the stability of the mode, without the need of numerical calculations.

# PART IV

## NUMERICAL RESULTS

- We study the stability of an $m = 1$, $n = -7$ tearing mode in the core of a RFP in the presence of a region of axial shear flow localized in the outer part of the plasma.

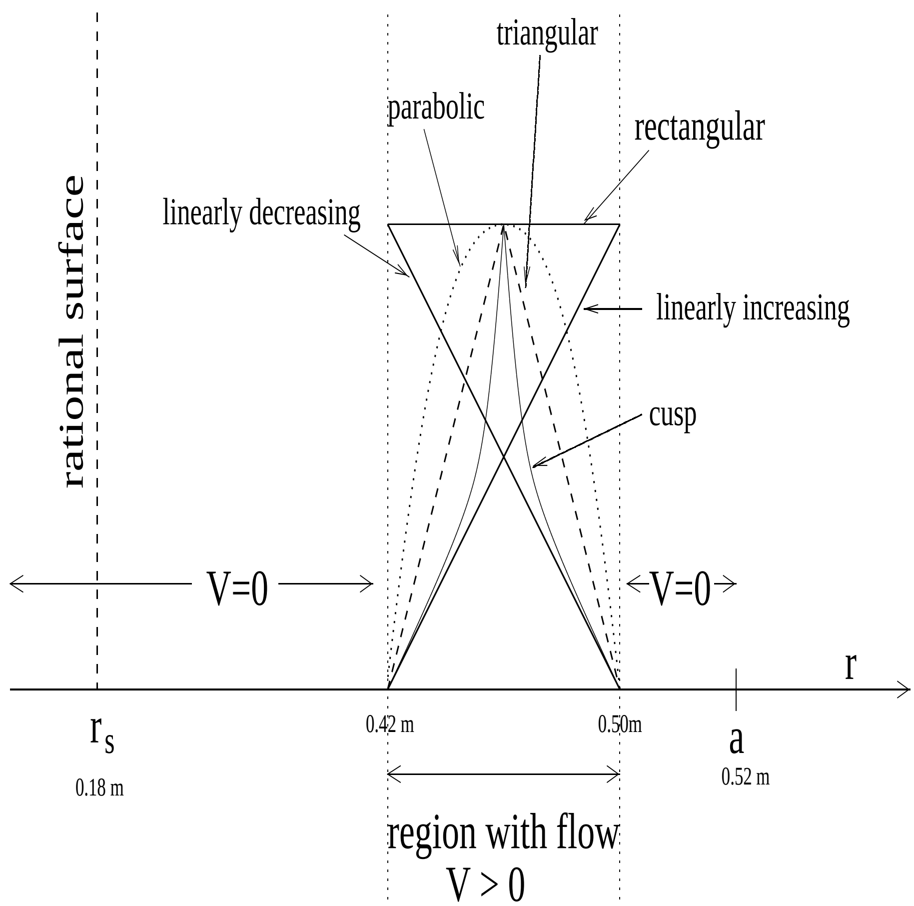


$V_z(r)$ flow profiles used in the simulations

# Reference configuration: $\Delta' = +0.485$

- The equilibrium profiles have been constructed from experimental data of a spontaneous enhanced confinement regime in MST

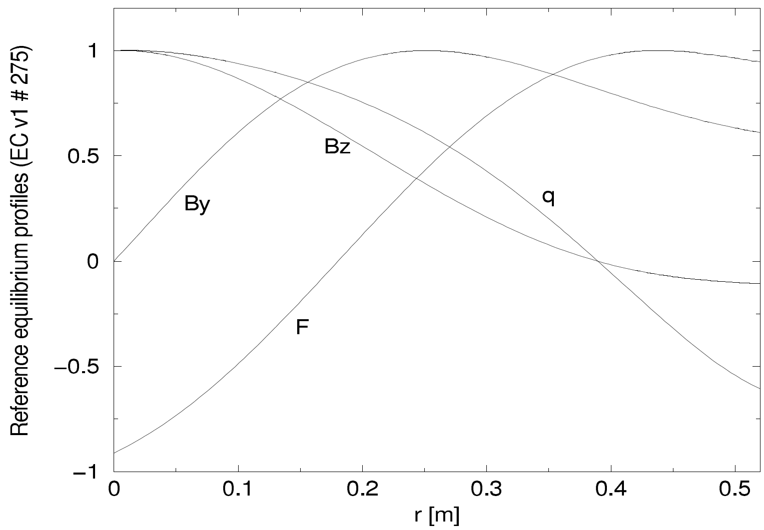


- Reference $B_r(r)$ eigenfunction ($r_s = 0.18$ m):

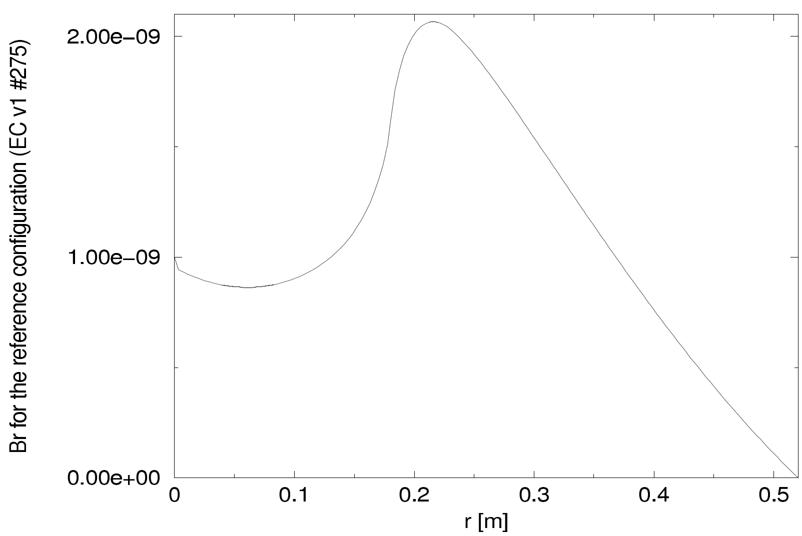

## Rectangular flow:

$$V_{z,max} = 0.3\ V_A,\ \ (V_{z,max}/L_V)/(V_A/a) = 1.95$$
$$\triangle' = +0.701$$

- $B_r(r)$ (compared to the no flow case):

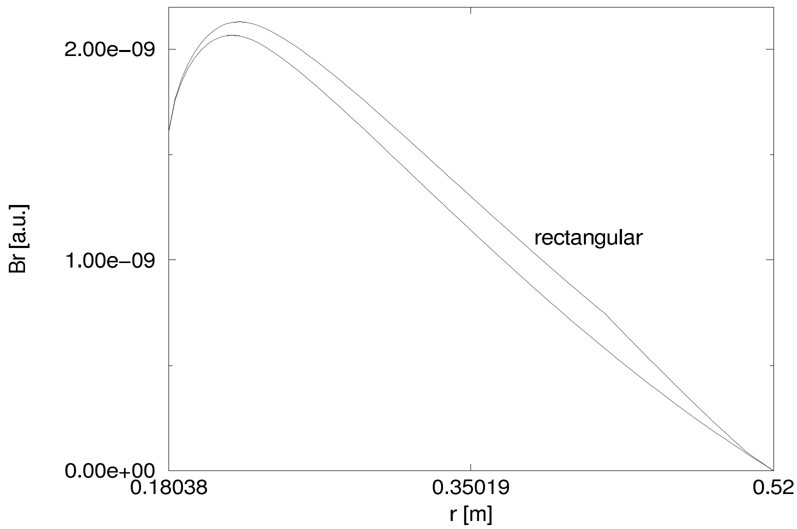


- $U_1(r)$ (compared with the flowless $U_0$)

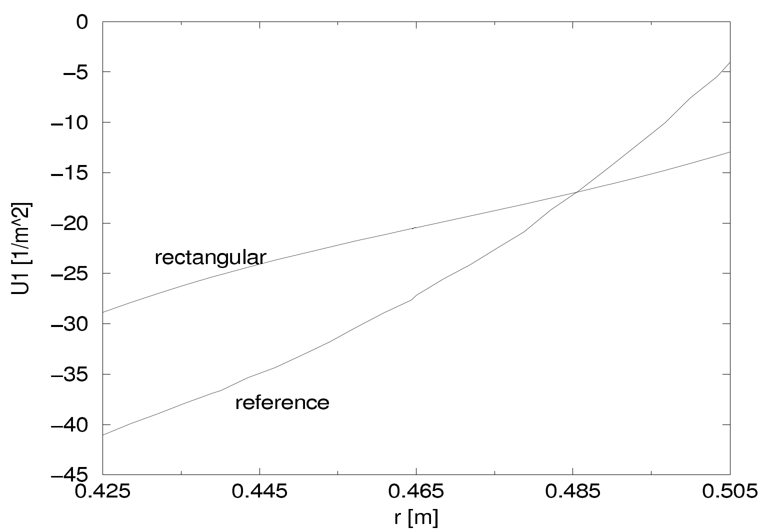

- Integrand in $\mathcal{I}$ [i.e., $r\ U_1\ [\psi/\psi(r_s)]^2$, with $\psi$ evaluated using the reference (no flow) eigen-function:

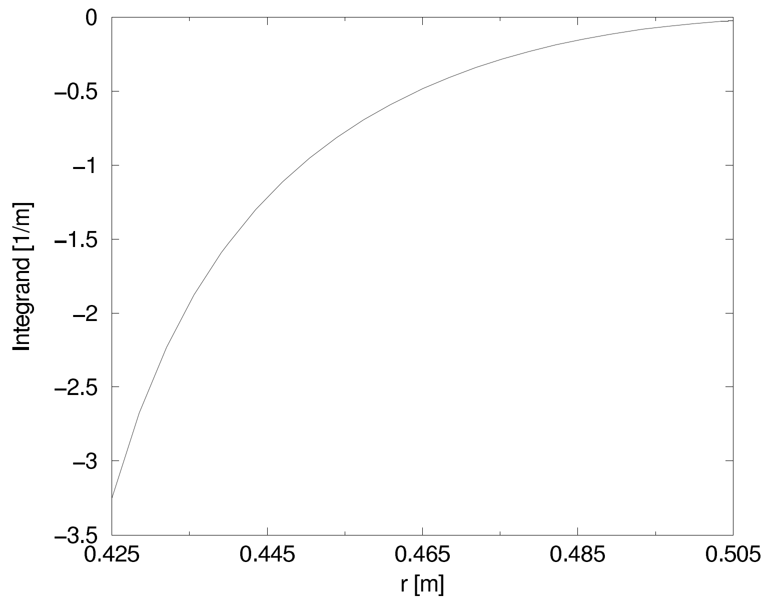


$U_1(r) < 0\ , \mathcal{I} < 0$ : *flow increases* $\Delta'$, *consistent with numerical result.*

<u>Linearly decreasing and increasing flows:</u>

$V_{z,max} = 0.6\ V_A$, $(V_{z,max}/L_V)/(V_A/a) = 3.90$

$\Delta' = +1.487$ and $\Delta' = 0.911$

- $B_r(r)$'s (compared with no flow case):

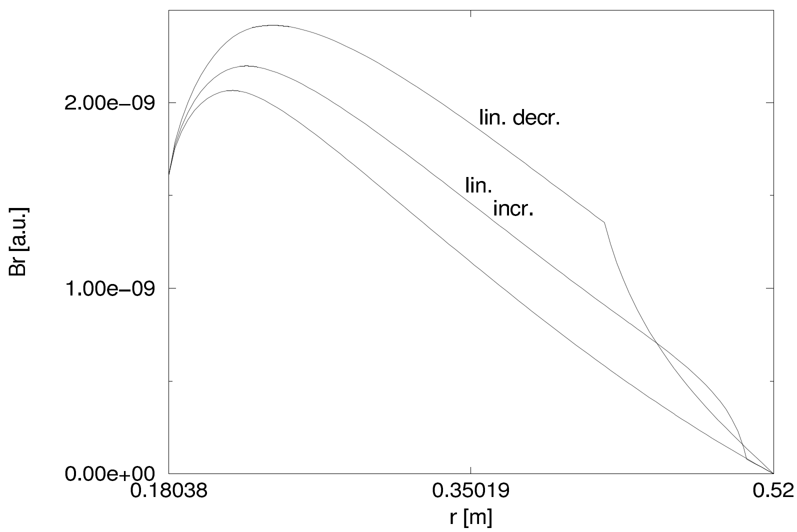


- $U_1(r)$:

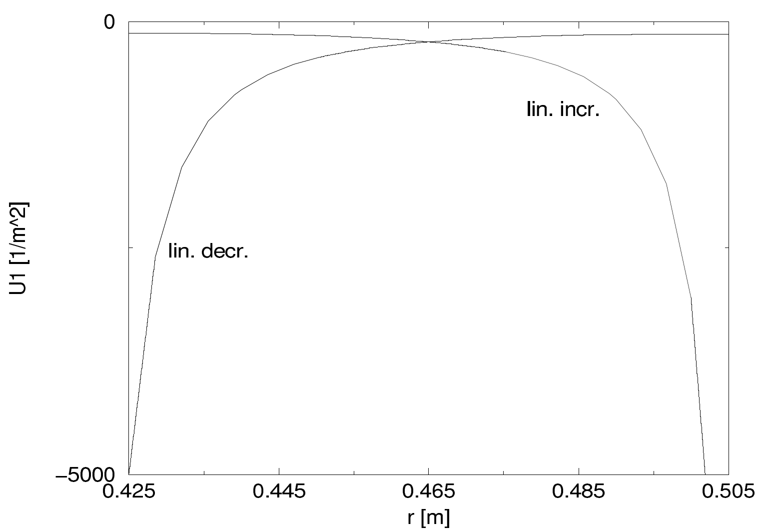

• Integrand in $\mathcal{I}$ [i.e., $r\ U_1\ [\psi/\psi(r_s)]^2$, with $\psi$ evaluated using the reference (no flow) eigenfunction:

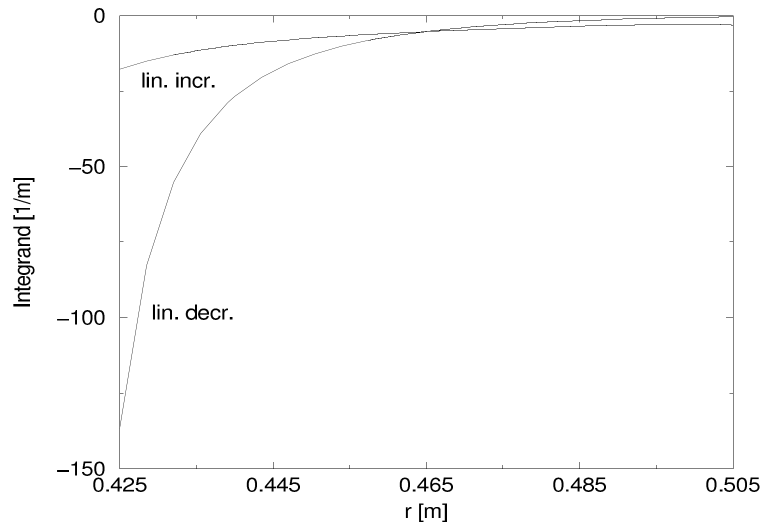


$U_1(r) < 0$ , $\mathcal{I} < 0$ : *flow increases* $\Delta'$, consistent with numerical result.

Also, $\mathcal{I}$ *more negative for linearly decreasing flow*, so that $\Delta'$ greater than for linearly increasing flow, consistent with numerical result.

<u>Triangular flow:</u>

$$V_{z,max} = 0.6\ V_A,\ \ (V_{z,max}/L_V)/(V_A/a) = 3.90$$
$$\triangle' = +0.913$$

- $B_r(r)$ (compared with no flow case):

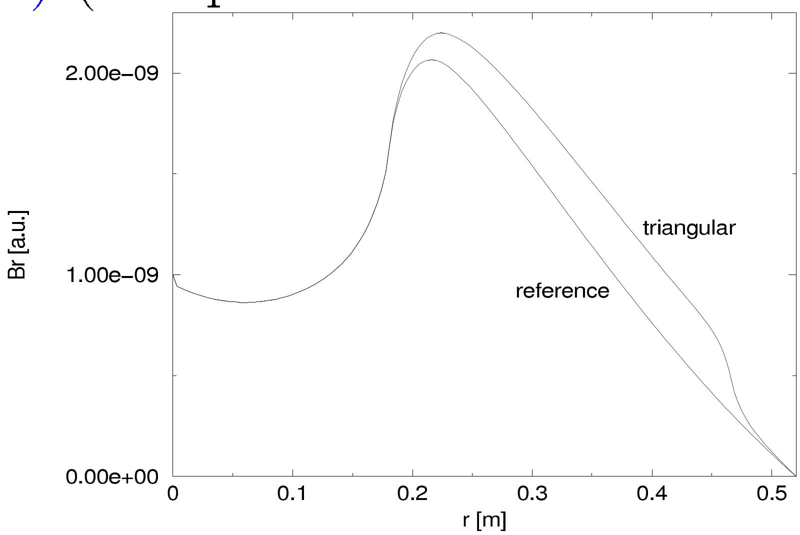


- $U_1(r)$:

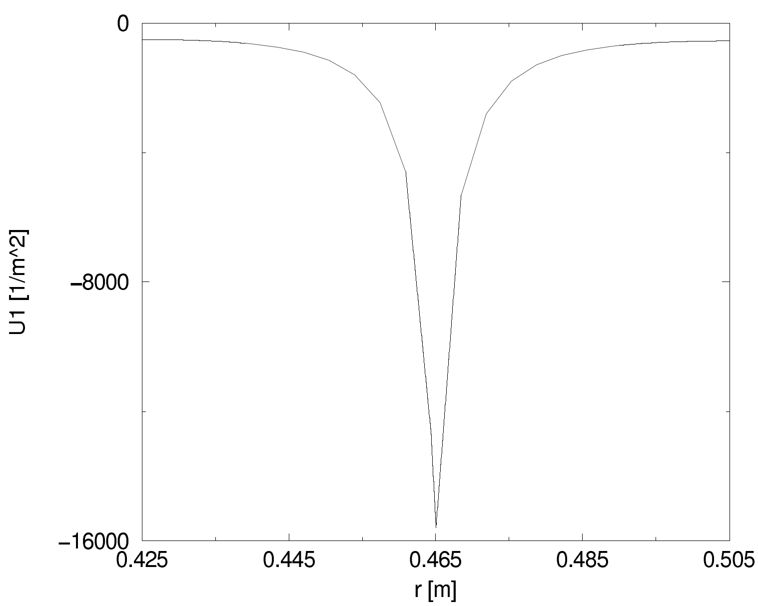

Parabolic flow:

$$V_{z,max} = 0.6\ V_A,\ \ (V_{z,max}/L_V)/(V_A/a) = 3.90$$
$$\Delta' = +1.736$$

- $B_r(r)$ (compared with no flow case):

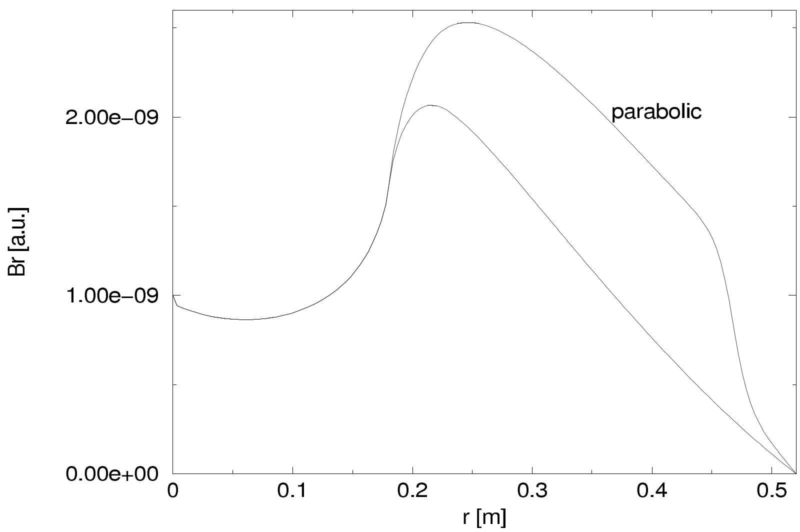


- $U_1(r)$:

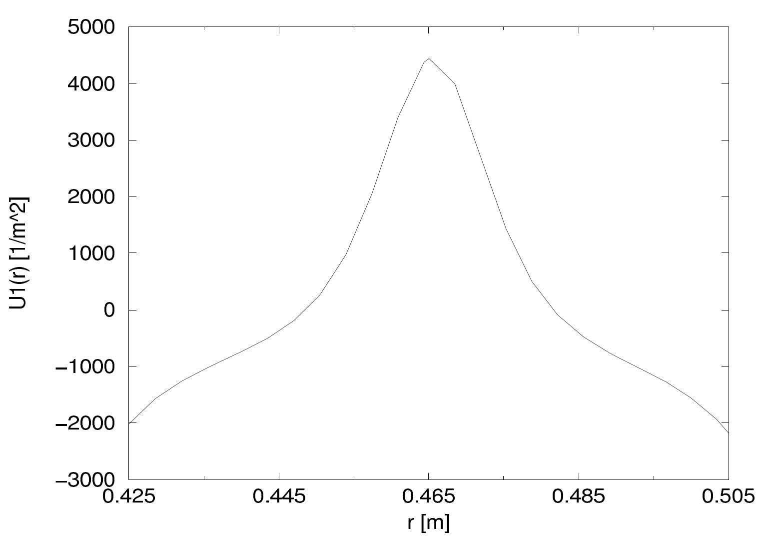

• Weighting function $r\ [\psi/\psi(r_s)]^2$ in the integral $\mathcal{I}$, with $\psi$ evaluated using the reference (no flow) eigenfunction:

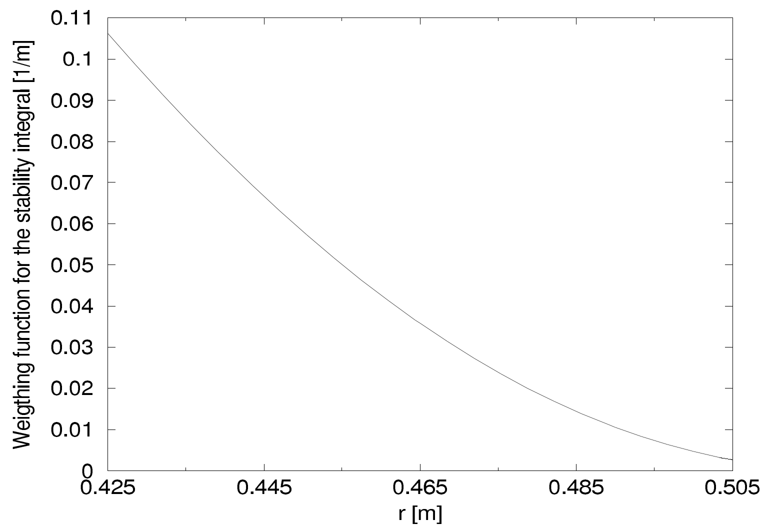


• Integrand in $\mathcal{I}$ [i.e., $r\ U_1\ [\psi/\psi(r_s)]^2$, with $\psi$ evaluated using the reference (no flow) eigenfunction:

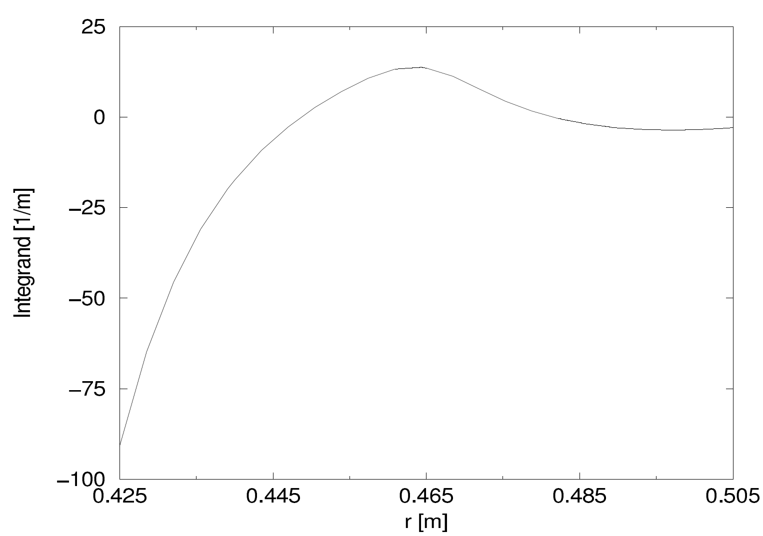

## Cusp flow:

$$V_{z,max} = 0.6\ V_A,\ \ (V_{z,max}/L_V)/(V_A/a) = 3.90$$
$$\Delta' = +0.711$$

- $B_r(r)$ (compared to no flow case):

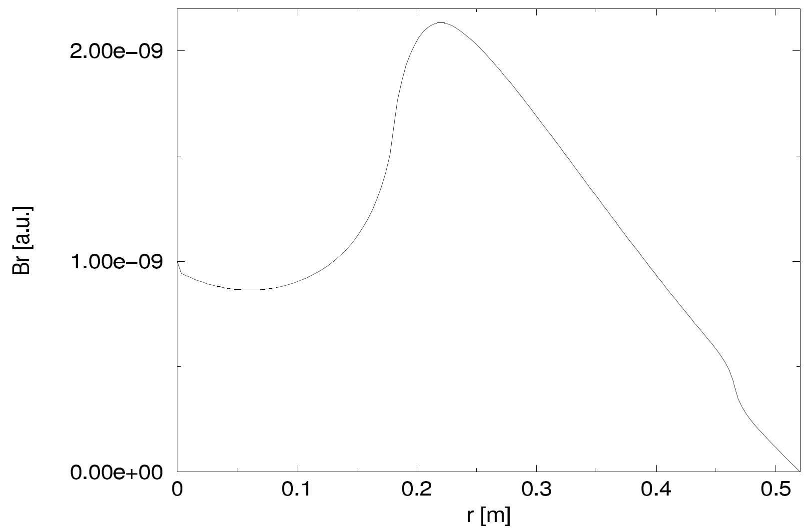


- $U_1(r)$:

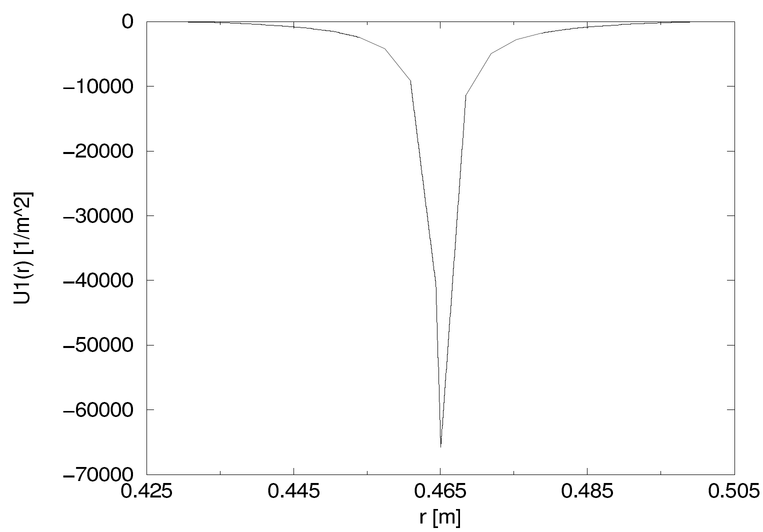


Flow profile narrower than parabolic case $\Rightarrow$ smaller increase in $\Delta'$.

# Flow location study (triangular flow)

- Stability factor vs central flow location:

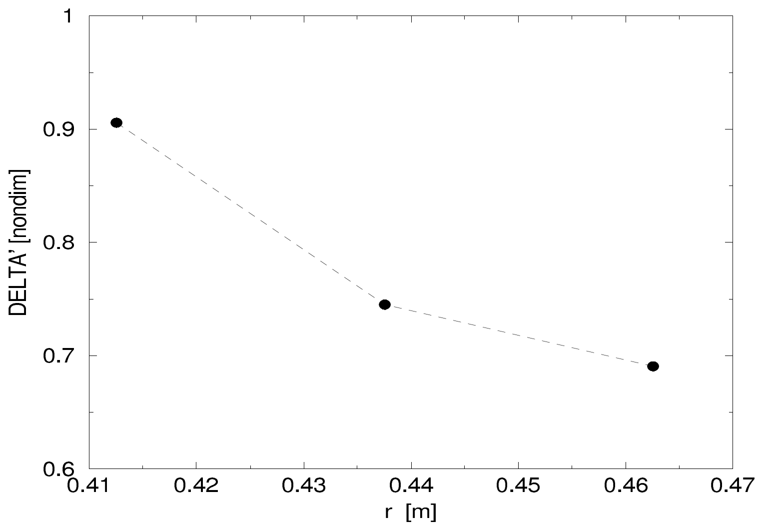


The localized triangular flow profile is more destabilizing the closer it is to the rational surface of the mode.

# PART VI

## CONCLUSIONS

- We have investigated numerically the influence on the stability of $m = 1$ core tearing modes in the reversed-field pinch of a region of axial shear flow localized away from the rational surface

- Jet-like flow profiles localized in the outer region of the plasma all further destabilize $m = 1$ modes

- The increase in $\Delta'$ is of order $(V_{z,max}/L_V)/(V_A/a)$ ($L_V$ = width of flow region)

- Numerical results agree with analytical predictions based on a "pseudo-potential energy" for the plasma

# Discussion

- Reduction of magnetic turbulence observed in the spontaneous enhanced confinement regime in the MST RFP is not due to flow shear stabilization of $m = 1$ modes
- Reduction of magnetic turbulence in improved RFP regimes could be due to:
  - $m = 0$ stabilization: flow shear is present in both outer and inner layer. Shear flow inside the inner layer is known to be stabilizing for large enough shear *[Chen and Morrison, Phys. Fluids B 2, 3, p.495, (1990)]*
  - indirect effects (e.g., change in current profile due to a reduction of edge resistivity, induced by shear flow stabilization of edge electrostatic modes)

# FUTURE WORK

- Consider the effect on $m = 1$ modes of other flow profiles:
  - $\tanh(r)$ and $\exp(r)$ flow profiles
  - flow profiles consistent with those induced by magnetic Reynolds stress at the $m = 0$ location

- Investigate the influence on the $m = 0$ mode of a region of shear flow localized on either sides of the rational surface

*This poster will be soon available at:*
*http://sprott.physics.wisc.edu/theory/home.htm*